JACS
JOURNAL OF THE AMERICAN CHEMICAL SOCIETY
ARTICLE
pubs.acs.org/JACS

−NH− Termination of the Si(111) Surface by Wet Chemistry

Fangyuan Tian, Douglass F. Taber, and Andrew V. Teplyakov*

Department of Chemistry and Biochemistry, University of Delaware, Newark, Delaware 19716, United States

Supporting Information

ABSTRACT: For over a quarter of a century the hydrogen-terminated Si(111) single-crystalline surface has been the gold standard as a starting point for silicon surface modification chemistry. However, creating a well-defined and stable interface based on Si−N bonds has remained elusive. Despite the fact that azides, nitro compounds, and amines do lead to the formation of surface Si−N, each of these modification schemes produces additional carbon- or oxygen-containing functional groups that in turn react with the surface itself, leaving contaminants that affect the interface properties for any further modification protocols. We describe the preparation of a Si(111) surface functionalized predominantly with Si−NH−Si species based on chlorination followed by *the room temperature* ammonia treatment utilizing NH_3-saturated tetrahydrofuran (THF). The obtained surface has been characterized by infrared spectroscopy and X-ray photoelectron spectroscopy. This analysis was supplemented with DFT calculations. This newly characterized surface will join the previously established H−Si(111) and Cl−Si(111) surfaces as a general starting point for the preparation of oxygen- and carbon-free interfaces, with numerous potential applications.

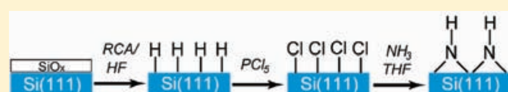

INTRODUCTION

Herein we report a method for preparing a Si(111) surface terminated with −NH− functionality by a wet chemistry approach consisting of chlorination followed by *the room temperature* treatment *with ammonia-saturated solvent*.

Elemental group IV semiconductors have had a tremendous impact on the development of science and technology for over half a century. As surface preparation for these materials started to play more and more influential role in the performance of modern devices, detailed protocols for the preparation of chemically functionalized semiconductors started emerging. Arguably, the hydrogen-terminated Si(111) single-crystalline surface has had the most impact and has been the gold standard as a starting point for silicon modification chemistry. Although this surface following its preparation is susceptible to oxidation under ambient conditions, it has proven to be sufficiently stable for chemical transformations leading to a remarkably versatile set of linkages. These methods include halogenation (−Cl and −Br),[1] alkylation to form Si−C bond by reacting with 1-alkene through hydrosilylation induced by thermal activation[2,3] or UV-irradiation,[4,5] functionalization with *n*-aldehydes and alcohols to form Si−O−C self-assembled monolayers (SAMs),[6,7] and a number of other approaches.[8−10] In addition, it was discovered that chlorinated silicon surfaces could react with Grignard reagents,[11] thiols,[12] and amines.[13]

Despite the fact that azides,[14,15] nitro compounds,[16−19] nitrosocompounds,[19] and amines[20−27] do lead to the formation of surface Si−N on clean silicon, each of these modification schemes introduces additional carbon- or oxygen-containing functional groups that in turn react with the surface itself, leaving contaminants that affect the interface properties for any further modification protocols. More importantly, these currently available approaches to generate Si−N surface species lead to a variety of products, making the design of uniform attachment schemes or contaminant-free interfaces with these surfaces as a starting point essentially impossible. A well-defined and stable Si−N interface free from oxygen and carbon could be important from both a fundamental and an applied standpoint. It should be pointed out that such a surface could provide the means to build thin films and self-assembled monolayers without commonly used Si−C bonds that are susceptible to oxidation, while providing a versatile functionality for chemical modification leading to a wide range of interfaces used in applications from solid diffusion barrier films to biocompatible sensors. It could be used for fabricating electronic devices (such as MOSFETs and MEMS[28]), and to enable the design of a variety of multilayer structures for yet undiscovered future applications.

Some of the recent success in providing the desired amino functionality is based on the reactions of ammonia with a clean silicon surface in ultrahigh vacuum (UHV). For example, ammonia reaction with a clean Si(100)-2 × 1 surface produces selectively $Si-NH_2$ and Si−H species in UHV conditions at room temperature.[29−39] With temperature increasing to 500 K, $Si-NH_2$ species start decomposing, which results in the insertion of the N atom to the neighboring Si−Si dimer and the formation of $(Si)_2NH$.[40] However, the clean Si(100)-2 × 1 surface cannot be handled outside the UHV conditions. So far the possibility to prepare oxygen- and carbon-free silicon surfaces uniformly terminated with $-NH_x$ functionalities by wet chemistry methods has remained elusive.

On the other hand, high-quality H-terminated silicon surfaces can be prepared by wet chemistry methods and are stable for some time under ambient conditions. Recent detailed vibrational and mechanistic computational studies by Chabal's group[41]

Received: June 3, 2011
Published: November 14, 2011

 © 2011 American Chemical Society

indicated that H-terminated Si(111) can react with gas-phase ammonia. The thermal reaction became rather complex at elevated temperatures. This reaction was shown to occur on an atomically flat H−Si(111) surface, but depended substantially on the surface morphology and defect structure. Exposing a hydrogen-terminated Si(111) surface to gas-phase ammonia formed $Si-NH_2$ at first at 350 °C, then with temperature increasing to 400 °C the N atom inserted into Si−Si framework to produce a $Si-NH_x$ layer.

If a chlorinated surface were used instead of H-terminated Si(111), the reaction with ammonia would be expected to occur substantially more readily than for H-terminated Si(111). It is known that the reaction of gas-phase[42,43] or liquid ammonia[44] and also primary and secondary amines[45,46] with chlorosilanes is extremely facile. Ammonia has been used with high selectivity in cyclocondensation and condensation reactions with several different compounds containing Si−Cl bond.[47−49] The ammonia reaction with surface $-O-SiHCl_2$ groups[50] and the formation of silicon nitride films from SiH_2Cl_2 and ammonia[51] suggest that this facile reaction should be versatile and adaptable to a variety of conditions.

Several surface functionalization schemes using chlorinated Si(111) surface as a starting point have already been developed. One of the main problems commonly encountered is the effect of water and oxygen on the quality of the surface produced. The chlorine atoms on the silicon surface withdraw electron density from silicon, making the surface susceptible to nucleophilic reactions. Ammonia appeared to be a great candidate for such a process, as long as it did not have to compete with oxygen-containing nucleophiles. Finstad et al.[52] showed that under UHV conditions ammonia reacted with the Cl−Si(100) surface to form primary amine and chlorine atom ($NH_2-Si-Si-Cl$) at lower temperature. With the temperature increased to 500−700 K, secondary amines were produced. Finally, at 1100 K silicon nitride is formed. The mechanism of the adsorption of ammonia on a chlorinated Si(100) surface was studied through density functional theory (DFT) calculations. The reaction between gas-phase NH_3 and Cl−Si(100) was predicted to produce a primary amine-terminated silicon surface and gas-phase HCl in an endothermic process.[53] A UHV study of several primary amines on a chlorinated Si(100) surface and a solution study of chlorinated porous silicon by Bergerson et al.[13] suggested that it is possible to replace surface chlorine atoms in a reaction with a primary amine. Although the chlorine-terminated Si(100) surface or porous silicon is certainly not as well-defined chemically as Cl−Si(111), the proposed reactions of amines with these substrates can serve as a guideline for understanding similar reactions on a Cl−Si(111) surface.

A recent comparative study of the gas-phase ammonia reaction on different halogenated Si(100) surfaces also warns against blocking effects of the reaction products that may remain on a surface and confirms that this type of a reaction should proceed via a penta-coordinated silicon intermediate.[54] The same study compared the process on H-terminated Si(100) and Cl-terminated Si(100) surfaces and suggested that the overall barrier on the former is substantially higher than on the latter.

In contrast to Si(100), little research has been done to show the reaction or mechanism of ammonia adsorption on chlorinated single-crystal Si(111) surfaces as prepared by wet chemistry. It should be advantageous to study this reaction on Si(111) surfaces, because the starting point for chlorination, the hydrogen-terminated silicon surface, is well-defined with nearly every single Si−H bond oriented perpendicular to the surface plane.

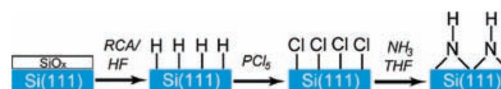

Figure 1. Schematic representation of the preparation steps to form a Si(111) surface terminated with Si−NH−Si functional groups.

Each Si−H reactive site on the Si(111) surface is occupied by *mono*-hydride, which is different from the H−Si(100) surface that normally has mono-, di-, and even trihydride species present.[10,55,56] Chlorination of H−Si(111) surface with PCl_5 has been demonstrated previously by Lewis et al.[11,57−59] A 99% surface coverage of chlorine can be reached, with every monohydride site substituted by a chlorine atom. The higher bond strength for Si−Cl (3.9 eV) compared to that of Si−H (3.3 eV) suggests that thermodynamics drives this transformation toward surface chlorination. Thus, it appears that Cl-terminated Si(111) substrate in a reaction with ammonia could deliver a carbon- and oxygen-free aminated surface. However, a strategy for running such a reaction while avoiding surface oxidation was needed.

In this present work, the reaction of ammonia-saturated THF with chlorinated Si(111) surfaces was investigated. We report the preparation (based on chlorination followed by ammonia treatment) of a predominantly Si−NH−Si-terminated Si(111) surface, as shown in Figure 1. Using the solvent saturated with ammonia allows us to run this reaction at room temperature, as opposed to the reaction with liquid ammonia that would require cryogenic conditions.[44] The solvent provides unique versatility from the practical perspective for running the synthetic modification under controlled conditions, especially when highly reactive and somewhat difficult to handle ammonia is used.[60−63] ***It should be noted that this room-temperature ammonia treatment avoids the thermal desorption of hydrogen from silicon and the silicon nitride formation that are observed at temperatures that are hundreds of degrees higher***.

We utilized infrared spectroscopy (IR) to investigate the changes of an Si−H monohydride site following chlorination, and then following ammonia treatment. X-ray photoelectron spectroscopy was used to confirm the formation of Si−Cl, and then, after exposure to ammonia, to distinguish primary, secondary, and tertiary amine species. Quantitative analysis of the XPS data was used to interrogate the surface coverage of chlorine and the products of ammonia treatment. Time-of-flight secondary ion mass spectroscopy (ToF-SIMS) was employed to investigate the surface species formed on a silicon surface after ammonia treatment. Finally, density functional theory (DFT) cluster calculations were performed to compare with the experimental XPS observations and to offer possible mechanisms of ammonia reaction with a chlorinated Si(111) surface.

■ EXPERIMENTAL SECTION

Materials. The n-type double-side polished Si(111) wafers (>0.1 ohm-cm resistance, 500 μm thickness) were obtained from Virginia Semiconductor. All chemicals were reagent grade or better and used as received: ammonium hydroxide (Fisher, 29% certified ACS plus grade), hydrochloric acid (Fisher, 37.3% certified ACS grade), hydrogen peroxide (Fisher, 30% certified ACS grade), buffer-HF improved (Transene Company, Inc.), chlorobenzene (Acros), PCl_5 (Aldrich), benzoyl peroxide (Acros), liquid ammonia (BOC Group), and THF (Fisher, distilled from Na/benzophenone). The deionized water used to rinse the surfaces and containers was from a first-generation Milli-Q water system (Millipore) with 18 MΩ·cm resistance.

Experimental Details. *Preparation of Hydrogen-Terminated Si(111) Surface.* The hydrogen-modified Si(111) surface was prepared by a modified RCA cleaning procedure.[64] The Teflon beakers and Si(111) wafers were cleaned in a solution of 4:1:1 Milli-Q water, hydrogen peroxide, and ammonium hydroxide for 30 and 10 min, respectively on an 80 °C water bath. After rinsing with Milli-Q water, the clean wafer was etched in HF buffer solution for 2 min and rinsed again with Milli-Q water. Then, the wafer was placed in a freshly prepared solution of 4:1:1 Milli-Q water, hydrogen peroxide, and hydrochloric acid for 10 min to grow a silicon oxide layer. After that, the rinsed wafer was etched in HF buffer solution again for 1 min, followed by 6 min in ammonium fluoride solution to form a well-ordered hydrogen-terminated Si(111) surface.

Preparation of Chlorine-Terminated Si (111) Surface. The chlorine-terminated Si(111) surface was prepared by a previously described procedure using PCl_5.[58] The solution of PCl_5 in chlorobenzene solvent with trace amount of benzoyl peroxide as reaction initiator was bubbled through with nitrogen gas under N_2 atmosphere for at least 30 min to remove gaseous impurities. This procedure was performed in a Schlenck tube without using a glovebox. A hydrogen-terminated Si(111) wafer was placed into this solution immediately after being blown dry with N_2. The entire setup was placed in an oil bath at 105 °C for 1 h to prepare the stable chlorine-terminated Si(111) sample.

Preparation of Amine-Functionalized Si(111) Surface. The freshly prepared chlorine-terminated Si(111) sample was immediately transferred into an ammonia-saturated THF solution in a water bath at room temperature. The ammonia/THF solution was prepared by condensing liquid ammonia with a dry ice−acetone cold trap into distilled THF. This solution was then warmed to room temperature in a water bath under N_2. The chlorinated silicon wafer was stirred in the ammonia/THF solution for 1 h to form an NH_x-terminated Si(111) surface.

Characterization Techniques. *X-ray Photoelectron Spectroscopy (XPS).* The XPS spectra were collected on a PHI-5600 instrument with a monochromatic Al Kα anode at energy of 1486.6 eV. The measurements were performed in a vacuum chamber with a base pressure of 1×10^{-9} Torr. The takeoff angle was 45° with respect to the analyzer. The survey spectra were collected over the energy range of 0−1000 eV. The high-resolution spectra for each element, Si 2p, O 1s, C 1s, Cl 2p, Cl 2s, and N 1s were collected over the range of 20 eV using an X-ray voltage of 13.5 keV at 0.1 eV/step. The data analysis was performed using Casa software. All peak positions and relative sensitivity factors were calibrated to the C 1s peak, which was taken to have the binding energy of 284.6 eV.

Quantification of surface coverages of chlorine and ammonia was performed on the basis of both survey and high-resolution spectra by applying the substrate−overlayer model. This model was proposed by Briggs and Seah,[65] and described in detail by Lewis' group.[66,67] Two assumptions were utilized: (1) chlorine- or nitrogen-containing groups are the closest to silicon substrate, and the adventitious hydrocarbon and oxygen layer is on top of the chlorine or nitrogen overlayer; (2) all the chlorine or nitrogen atoms in the overlayer are in the solid state. The equivalent monolayer coverage of an overlayer species was calculated from the relationship:

$$\Phi_{\mathrm{Ov}} = \left[\left(\frac{\lambda \sin \Theta}{a_{\mathrm{Ov}}}\right)\left(\frac{SF_{\mathrm{Si}}}{SF_{\mathrm{Ov}}}\right)\left(\frac{\rho_{\mathrm{Si}}}{\rho_{\mathrm{Ov}}}\right)\left(\frac{I_{\mathrm{Ov}}}{I_{\mathrm{Si}}}\right)\right] \quad (1)$$

where Φ is the overlayer coverage; λ is the penetration depth (2.0 nm in this instrument at 45° takeoff angle); θ is the photoelectron takeoff angle with respect to the analyzer (45°); a_{Ov} is the atomic diameter of the overlayer species. a_{Ov} was calculated by the following equation:

$$a_{\mathrm{Ov}} = \left(\frac{A_{\mathrm{Ov}}}{\rho_{\mathrm{Ov}} N_{\mathrm{A}}}\right)^{1/3} \quad (2)$$

where A_{Ov} is the atomic weight of the overlayer species: 35.45 and 14.01 for Cl and N atoms, respectively; and N_{A} is Avogadro's constant. SF is the sensitivity factor: 0.90, 2.38, 1.70, and 1.69 for the Si 2p, Cl 2p, Cl 2s, and N 1s peaks, respectively. ρ is the volumetric density, also called atomic density: 2.0, 1.26, and 2.328 g/cm^3, or 3.43×10^{22}, 5.41×10^{22}, and 5.0×10^{22} atom/cm^3 for the Cl, N, and Si atoms, respectively.[68] I is the integrated area under the overlayer or substrate peaks, as determined by Casa XPS software.

Fourier-Transform Infrared Spectroscopy (FTIR). Single beam spectra were collected using a Nicolet Magna-IR 560 spectrometer with a liquid-nitrogen-cooled external MCT-A detector. The FT-IR spectra were collected in the range 4000−650 cm^{-1} with a 60° angle with respect to the incoming infrared beam. 512 scans per spectrum and a resolution of 8 cm^{-1} were used to collect all the spectra. The native oxide-covered and hydrogen-terminated Si(111) wafers were used as backgrounds, as indicated below.

Time-of-Flight Secondary Ion Mass Spectrometry (ToF-SIMS). A ToF-SIMS instrument (ToF-SIMS IV, ION-TOF, Münster, Germany) was used to obtain static negative and positive spectra with a 25 keV monoisotopic ^{69}Ga ion beam. The mass resolution was $m/\Delta m$ = 10,000, and the raster area of the Ga ion gun was 500 × 500 μm^2 with the resolution of 128 × 128 pixels. All primary gallium ion fluences were below the threshold of 1×10^{13} ions/cm^2 for static SIMS.

Computational Details. Density functional theory calculations were performed using the *Gaussian 09* suite of programs[69] with the B3LYP functional and 6-311G+(d,p) basis set.[70−73] A $Si_{17}H_{24}$ model including two Si−H reactive sites was used to compare with XPS observations and to explore the possible surface reaction mechanisms; the $Si_{21}H_{28}$ model with three reactive sites and the $Si_{10}H_{16}$ cluster with a single surface reactive site were used to confirm the first step of this mechanism, ammonia reaction with a chlorinated Si(111) surface. N 1s core-level energy in the models were predicted using Koopmans' theorem, and the correction factor to the predicted core-level energy for N 1s was found to be 8.06 eV on the basis of our previous investigations.[9] All of the predicted N 1s energies from calculations in this work were corrected by this factor and then compared with the experimental results.

RESULTS AND DISCUSSION

Since the goal of this study was to obtain a selectively NH_x-terminated Si(111) surface by wet chemistry methods, it was important to carefully follow each step in the preparation process spectroscopically to ensure that the desired surface termination is achieved. This also means that no single spectroscopic technique would be sufficient for a complete characterization of each modification step. As described below, we used vibrational infrared spectroscopy to follow the preparation of H-terminated Si(111), since the vibrational frequency of the Si−H stretch is extremely sensitive to surface order and even can be used to indicate the cleanliness of the preparation procedure. The same technique was also used to analyze the NH_x-terminated surface. XPS was further utilized to interrogate surface coverage for Cl- and NH_x-terminated silicon surfaces and ToF-SIMS was used to probe the chemical nature of surface-terminating species after the final modification step.

Infrared Studies. Figure 2 summarizes the selected results of infrared investigations of the N−H and Si−H stretching regions of the silicon samples following the modification steps and also shows the spectral region where $\delta(NH_2)$ vibrations are expected. The sharp Si−H stretching peak at 2083 cm^{-1}, a signature of a clean and well-ordered H−Si(111) surface shown in Figure 2a fully disappears after chlorination, as shown in Figure 2b, and is still absent following modification with NH_3 in anhydrous THF

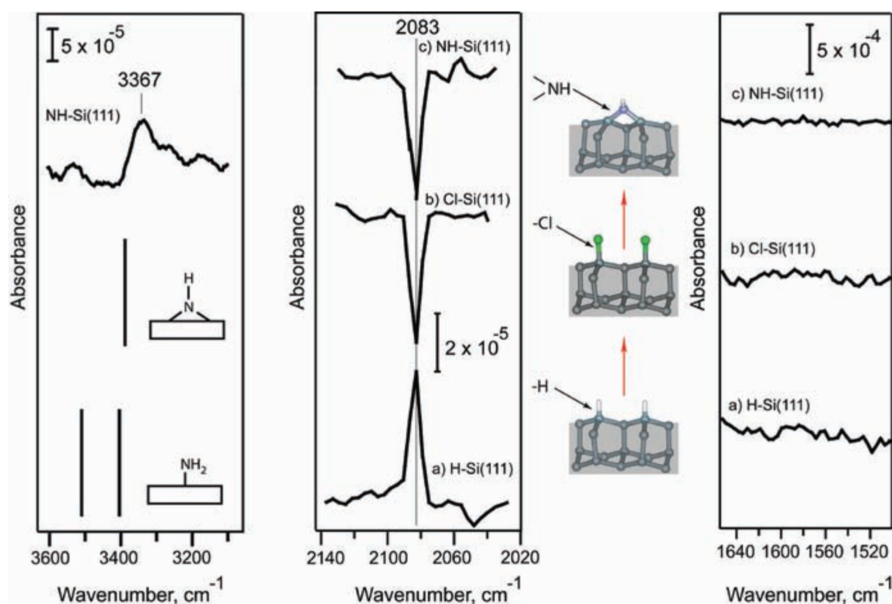

Figure 2. Transmission infrared spectroscopic studies of the Si(111) modification steps. The Si−H stretching and $-NH_2$ bending spectral regions are presented for (a) Si(111) surface terminated with hydrogen; (b) Cl-terminated surface prepared by exposure to PCl_5 in the presence of benzoyl peroxide initiator; (c) Si−NH−Si-terminated silicon surface prepared by exposure of Cl-terminated Si(111) to NH_3/THF. Spectra (a) use a clean silicon wafer covered with a thermal oxide as a background. Spectra (b) and (c) use a single beam spectrum collected in (a) as a background. Schematic representations of the proposed surface structures are provided on the basis of a computational cluster representing two neighboring surface silicon atom sites. Gray - silicon, green - chlorine, white - hydrogen, blue - nitrogen. In the cluster models, hydrogen atoms terminating silicon atoms representing subsurface are omitted for clarity. Left panel presents the N−H stretching region spectrum obtained on the basis of averaging five different experiments for better signal-to-noise ratio. The expected vibrational frequencies for surface −NH− and $-NH_2$ species obtained from computational models described below are presented as solid bars (frequencies are scaled by a common scaling factor of 0.965).

in Figure 2c. Since the changes in the position of this peak are very sensitive to the specific species observed on a surface, this can also be used as a gauge of a uniform reaction. It is important to note that nearly all the intensity of the Si−H stretch vibration has disappeared within the signal-to-noise ratio of our experimental setup. It is also important that nearly all the surface hydrogen available before chlorination step is replaced with chlorine.

It is well-known that the intensity of the stretch vibrations of submonolayer NH_x species on silicon is extremely small,[34,74] and this spectroscopic region is rarely used for precise identification of submonolayer species. Nevertheless, as shown in the left panel of Figure 2, we did observe a relatively broad and weak stretching vibrations corresponding to $-NH_x$ species around 3500 cm^{-1} following ammonia treatment. Although the position of the main observed feature at approximately 3367 cm^{-1} could be affected by the presence of impurities adsorbed on this surface at ambient conditions, it is clear that this major feature is consistent with the vibrational frequency expected for surface −NH− groups according to the computational result shown as a solid bar predicted for surface models described below. This experimental result is also in a drastic contrast with the doublet feature expected for symmetric and asymmetric N−H stretching vibrations of the $-NH_2$ group also illustrated in this figure. The presence of surface $-NH_2$ groups as a minority cannot be ruled out, given the signal-to-noise ratio in our experimental setup. In fact, some of the low-intensity features recorded around 3500 cm^{-1} could originate from such minority species. However, given that the absorption intensity for primary amine species is substantially higher than secondary amino groups investigated in similar chemical environments,[75,76] it is straightforward to infer that the majority of surface chemical groups present on this ammonia-modified surface in our experiments are −NH−. Even more importantly, no signature of NH_2 bending modes, which at comparable coverages could be easily observed in previous studies[41,77,78] was recorded for sample (c), as shown on the right panel of Figure 2, which is consistent with other analyses outlined below. Thus, the infrared spectroscopy suggests that we have formed a well-ordered and clean Si(111) surface terminated with hydrogen, removed all the hydrogen atoms during the chlorination step, and following modification of that chlorinated surface with ammonia in THF, surface −NH− species were the predominant product.

X-ray Photoelectron Spectroscopy Studies. In order to confirm the identity of the surface functional groups and to quantify the concentrations of the species present on the silicon surface following each modification step we used XPS to monitor N 1s, Cl 2s, Cl 2p, and Si 2p spectral regions. We also collected survey spectra for each sample studied. Representative Cl 2p spectra of the Si(111) surface before and after ammonia modification are given in Figure 3. Since only one type of chlorine-containing species is present on the surface following the modification of the H−Si(111) sample with PCl_5 in the presence of benzoyl peroxide, as evidenced in Figure 3a, and since the infrared signature of hydrogen present on this surface disappears following chlorination as shown in Figure 2, it is reasonable to assume that a fully chlorinated Cl−Si(111) surface had been prepared following the second step outlined in Figure 1. To confirm this assumption, quantitative analysis of the XPS spectra was performed according to Lewis et al.[58] We observed a very similar value of the corrected intensity ratio between Cl 1s and Si 2p, corresponding to approximately 99% of the Si(111) surface sites occupied by chlorine atoms.

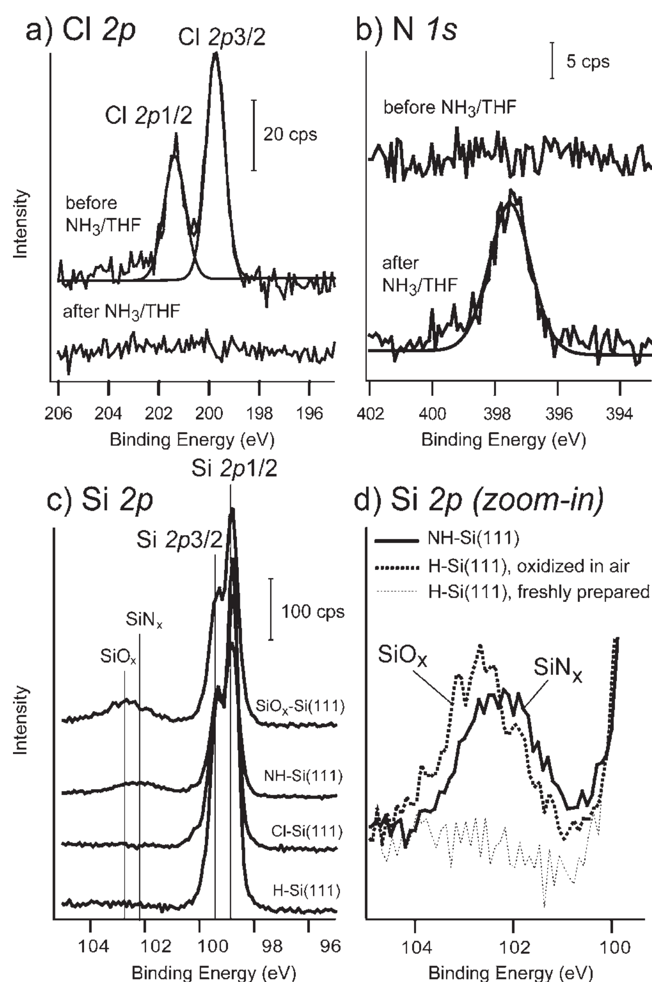

Figure 3. XPS spectra of the Si(111) surface before and after ammonia modification: (a) Cl 2p region; (b) N 1s region; (c) Si 2p region comparison for H- and Cl-terminated surface with those of Cl−Si(111) exposed to NH_3/THF treatment and also H−Si(111) left in air; (d) zoom-in of the SiN_x and SiO_x regions from (c), scaled for clarity.

We continued these studies after the exposure to ammonia in THF. We concluded that the N 1s feature at 397.6 eV in Figure 3b indicated a Si−NH−Si functionality. The binding energy that corresponds to the observed feature was compared to the DFT predictions, as explained in detail in the DFT calculation part. The computational value[9] of 397.6 eV for the model studied is in perfect agreement with the observed value. Even more importantly, any surface nitrogen oxidation would shift the observed peak by at least an electron volt toward *higher* binding energy, as also summarized in the DFT computational investigation below. This is consistent with a very minor peak observed above 399 eV, likely resulting from partial surface oxidation during sample transfer. The assignment of the main observed feature to Si−NH−Si, as opposed to Si−NH_2 is also based on a detailed study by Bishoff et al.,[79] who reported a shift of N 1s feature from 398.6 eV for Si−NH_2 species to 398.0 eV for Si−NH−Si species on model surfaces in ultrahigh vacuum. To further reinforce this assignment, quantitative analysis of the XPS spectra of the ammonia-modified silicon surface was performed. Comparison of the ratio of N 1s feature and Si 2p feature on the ammonia-treated surface with that of the Cl 2p feature and Si 2p feature on the Cl-covered Si(111) (where ∼99% of the surface is covered with Cl atoms) and utilizing the calibration approach described by N. Lewis et al.,[58,67,80] we determine that nitrogen coverage on the ammonia-exposed surface is approximately half that of chlorine on Cl−Si(111). The numbers based on repeated experiments with different samples yield 55 ± 9% as a ratio of nitrogen coverage on a treated Si(111) surface to chlorine coverage on Cl−Si(111). It should again be emphasized that according to the XPS data, all the chlorine is removed following ammonia treatment. Thus, in an exchange reaction, one Si−NH−Si group replaces two Si−Cl groups, consistent with the reaction scheme outlined in Figure 1.

The analysis of the Si 2p spectrum in Figure 3c further reaffirms these conclusions. There is no observable silicon surface oxidation during our experimental procedure for obtaining H-terminated and Cl-terminated Si(111) substrates. A spectrum obtained following NH_3/THF exposure exhibits a small feature at 102.2 eV in addition to the familiar signatures of the clean silicon surface. This feature corresponds to the minority SiN_x surface species. Although it could not be completely ruled out that it encompasses both surface SiO_x and SiN_x species, the majority of these species appear not to be affected by surface oxidation. To reassure that the spectroscopic signature of the surface nitrogen-containing minority species within the Si 2p spectral region is different from the species resulting from surface oxidation, Figure 3d zooms in the scaled spectral portion of the Si 2p region corresponding to surface oxides and nitrides. Clearly, the SiO_x species observed around 103 eV following H−Si(111) surface oxidation in ambient are different from the SiN_x species observed at 102.2 eV following NH_3/THF treatment of the Cl−Si(111) surface. In fact, even if the scaled feature corresponding to SiO_x species is subtracted from the Si 2p spectrum collected following ammonia treatment, the intensity corresponding to the minority SiN_x feature would still be at least 4 times higher compared to the SiO_x component. It may be difficult to separate the surface Si−NH_2 and Si−NH−Si species from the main features of bulk silicon in the Si 2p spectra. However, the small feature observed at 102.2 eV may be either the signature of a specific configuration of −NH− surface groups or possibly a sign of a silicon nitride formation, for example, at defect sites. It is worth emphasizing again that running the reaction at room temperature avoids the thermal removal of surface hydrogen and the formation of silicon nitride, as both these processes occur above 700 K. The surface obtained by the NH_3/THF treatment is stable in the vacuum of the XPS instrument, or for several days in anhydrous THF at room temperature. If a pure THF is used in this experiment without ammonia, no changes are observed to the Cl-terminated Si(111) surface. One important observation is that if the surface exposed to NH_3/THF were covered predominantly with NH_2-groups, the Si 2p region of the XPS spectra would be expected to exhibit a different shape, with a feature corresponding to a σ_{Si-N} bond appearing at approximately 101 eV.[81,82] However, zooming into the leading edge of the Si 2p peak helps to rule out this possibility, consistent with the conclusion that the surface produced by the ammonia treatment of the chlorinated Si(111) single crystal resembles surface silicon nitride (with −NH− functionality inserted into a Si−Si bond) more closely than the NH_2-terminated silicon. Thus, on the basis of the quantitative XPS analysis in combination with infrared studies, it can be concluded that nearly every hydrogen atom on an ideally ordered H−Si(111) surface is replaced by a chlorine atom following PCl_5 chlorination procedure. Following chlorination, ammonia treatment

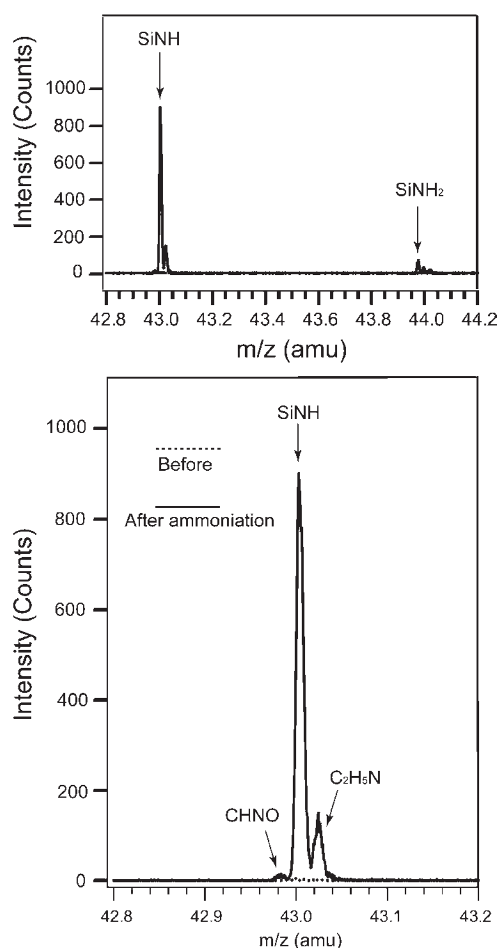

Figure 4. ToF-SIMS negative-ion spectrum of Si(111) surface after ammonia modification in the NH_x species range. The bottom panel is a zoom-in of the SiNH species spectral region with a comparison of the spectra before (dashed line) and after (solid line) ammonia modification.

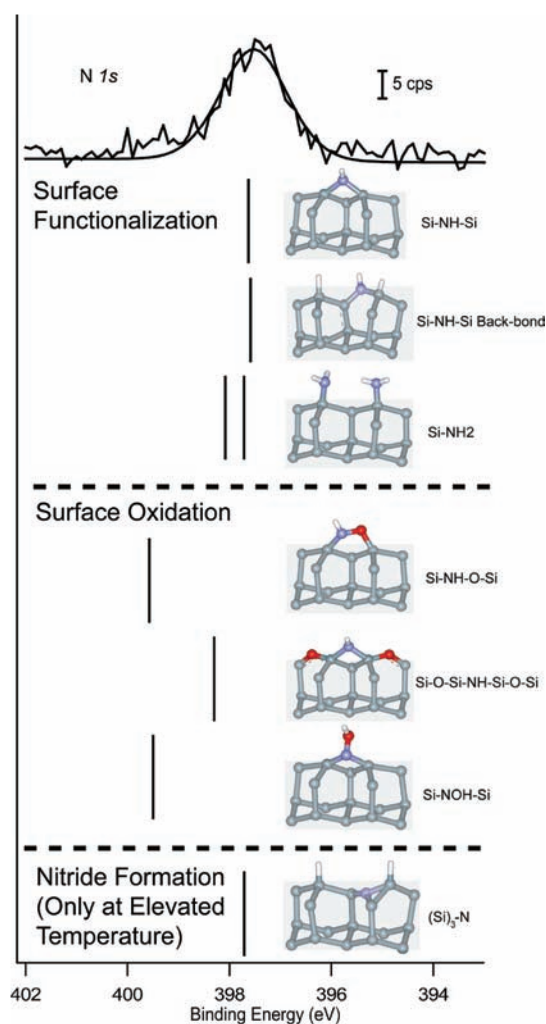

Figure 5. N 1s XPS spectrum of Si (111) surface following ammonia modification (top), and the N 1s core-level energies predicted by DFT calculations (solid bars) for the possible surface models. Surface functionalization is represented by the top three clusters, potential surface oxidation products are given by the next three models, the surface nitride formation pathway that is only possible at elevated temperatures is presented by the cluster at the bottom. Gray - silicon, white - hydrogen, red - oxygen, blue - nitrogen. In the cluster models, hydrogen atoms terminating silicon atoms representing subsurface are omitted for clarity.

replaces approximately every two surface chlorine atoms with one nitrogen. The functionality formed during ammonia treatment is not consistent with the presence of $-NH_2$ functional groups but rather with some structure that is more similar to surface nitride at nearly exactly half-monolayer coverage, or a structure of a general form of Si−NH−Si.

ToF-SIMS Studies. To verify the nature of the $-NH_x$ species present on a silicon surface following ammonia treatment we used the high sensitivity ToF-SIMS within a mass-to-charge range of 0−100 amu. Both positive and negative spectra were collected for the samples before and after ammonia treatment but only the negative ion spectra are shown in this paper since they are more reliable in identification of nitrogen compounds.[83] Figure 4 presents the intensity differences before and after ammonia treatment from 42.8 to 44.2 mass-to-charge range. The Si−NH signature clearly exhibits the highest intensity. Generally, ToF-SIMS cannot be used for a quantitative measurement of a difference between closely related surface species; however, if the ionization cross sections of the Si−NH and $Si-NH_2$ species are similar, the intensity difference between these species suggests that most of them are originated from Si−NH−Si and not from the $Si-NH_2$ surface species. To draw a quantitative conclusion based on these data, the exact nature of the surface species present, their arrangement on a surface, interaction with the incoming ion beam, and an ionization cross section of the resulting species would have to be known, but this observation serves as a supporting evidence of the majority of the species present on a silicon surface following the ammonia treatment being Si−NH−Si.

In agreement with the XPS spectra described above, and as summarized in the bottom panel of Figure 4, ToF-SIMS studies also indicate that, before the ammonia treatment, the intensity of all the NH_x-containing species coming from the surface is essentially zero. However, after the reaction with ammonia the $Si-NH_x$ was definitely formed, and these species are predominantly of the Si−NH−Si type. Due to the exposure to ambient conditions during the transfer process, minor carbon contamination was also detected, as shown in the same figure.

Computational Studies. From our XPS studies, only one major peak at a binding energy of 397.6 eV, shown in Figure 3b is

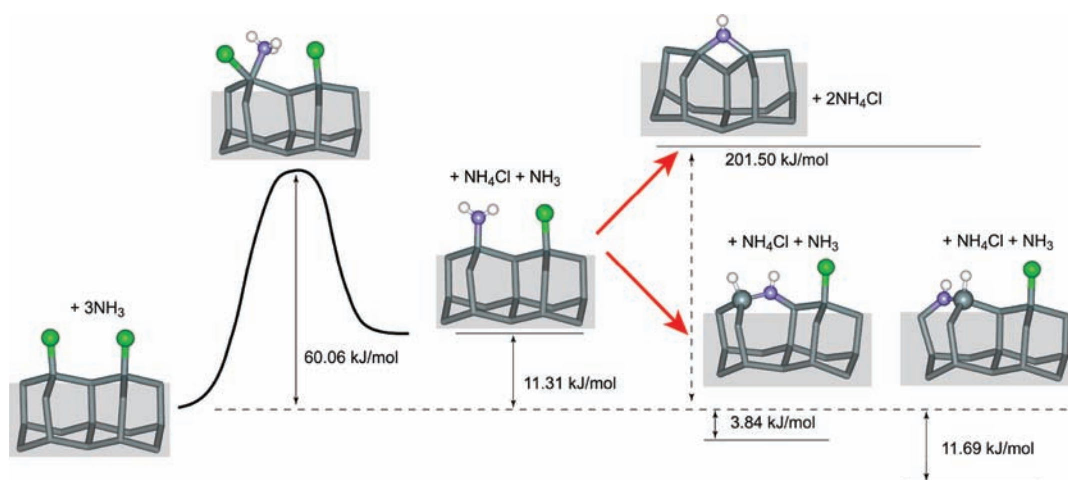

Figure 6. DFT investigation of possible mechanisms for the ammonia reaction with a Cl−Si(111) surface and possible surface reaction products following initial chlorine replacement by an $-NH_2$ group. The energies reported in kJ/mol were obtained with B3LYP/6-311+G(d,p) computational approach using $Si_{17}H_{24}$ model cluster with two hydrogen atoms connected to the topmost silicon (representing the surface) replaced by appropriate adsorbates. Gray - silicon, green - chlorine, white - hydrogen, blue - nitrogen. In the cluster models, hydrogen atoms terminating silicon atoms representing the subsurface are omitted for clarity.

observed in high-resolution N 1s spectrum. This symmetric peak was fitted by only one component, suggesting that only one *type* of nitrogen-containing surface functionality was formed. The observed binding energy is close to 398.0−398.1 eV, literature values for secondary amine.[37−39,41,52,84] Compared to the literature value of 398.7[79,85] reported for N 1s of a primary amine, the peak observed in this study is 1 eV lower, which suggests that it is highly unlikely that the majority species in our case is a primary amine. In order to confirm this statement, we used density functional theory to predict the binding energies of N 1s on the basis of different chemical models, including primary amine, secondary amine, and oxidized primary/secondary amine species.

All these computational studies are based on a cluster model representing the two closest topmost silicon sites on the unreconstructed Si(111) surface. Selected results of the DFT study are summarized in Figure 5. The predicted N 1s binding energy for two main possible Si−NH−Si geometries are 397.63 and 397.58 eV, which is the closest to the observed XPS value. The model with primary amine groups has two closely spaced N 1s binding energies around 398 eV. The difference in the predicted core level energies for primary and secondary amine groups that could be formed on a Si(111) surface is consistent with the experimental studies presented above. It does support the predominance of the Si−NH−Si species. More importantly, however, the studies of the model clusters representing possible surface oxidation pathways with oxygen atoms inserted into the Si−N linkage suggest that any of these species would cause the N 1s peak to shift by about 1 eV or even more to higher energy: the N 1s binding energy for Si−NH−O−Si model was predicted at 399.6 eV, and for Si−N(OH)−Si model was calculated to be 399.5 eV. Even when the oxygen atoms present on a surface are not directly connected to nitrogen, the core level energy shift would be expected to be easily observed in an experiment. In fact, a barely visible feature observed above 399 eV in our experiments most likely indicates the presence of oxidized surface species produced on a sample during the transfer, consistent with a minority species observed within the Si 2p spectral range. Thus, the comparison of experimentally observed N 1s features and the core level energies predicted computationally rules out the role of surface oxygen in determining the nature of the majority species on ammonia-modified surface.

Finally, some of the proposed structures containing the Si−NH−Si functionality may appear highly strained. Extended computational models should normally be employed to determine the mechanisms of surface reactions; however, several important characteristics of this mechanism can be established on the basis of the results of the computational studies involving model clusters, as summarized in Figure 6. First, the replacement of a surface Cl atom with an $-NH_2$ group is a slightly endothermic reaction with a low barrier. The excess of a reagent NH_3 shifts the equilibrium toward the formation of $-NH_2$-terminated surface kinetically, and the produced surface is expected to be stable under mild conditions. In addition to the $Si_{17}H_{24}$ cluster shown in Figure 6, we have also performed analogous calculations on a smaller model, $Si_{10}H_{16}$, and on a cluster model representing three neighboring surface reactive sites, $Si_{21}H_{28}$, to confirm that the first step of the proposed mechanism is not substantially affected by the neighboring chlorine atoms. All the results are consistent, and additional computational studies are presented in the Supporting Information section. Following this first reaction step, the newly formed $-NH_2$ group could react with a neighboring surface chlorine atom. This reaction can proceed by HCl elimination and the formation of a bond between the nitrogen atom and the topmost silicon atom from which the chlorine was eliminated. However, as suggested by the model, this pathway would be unfavorable thermodynamically, even though it is possible that this structure could be formed at room temperature. On the other hand, if chlorine elimination is accompanied by the insertion of the −NH− entity into the Si−Si backbond, thermodynamics of such a process is slightly exothermic, as illustrated in Figure 6. More extended structure calculations should be employed to uncover the details of the mechanism and further surface transformations but it seems that the backbonded −NH− functionality is the most likely termination of the Si(111) surface prepared by the ammonia treatment following chlorination. If this process created an additional dangling bond following chlorine elimination, another ammonia molecule could adsorb

and react on such a site, possibly reflecting a slightly higher than 0.5 coverage of the $-NH_x$ groups produced, as observed in our experiments. Thus, it is clear that a number of additional studies will be needed in the future to assess the long-range arrangement of surface species and to determine the mechanism of nitrogen insertion process. Further computational investigations of this reaction should examine the role of coverage, defects, adsorbate–adsorbate interaction and partial monolayers with various coadsorbed species, such as $-NH_2$ and $-NH-$. It has been shown that the effects of coadsorbates could alter the stability and energy barriers in similar insertion processes on Si(100) by hundreds of kJ/mol and these profound effects should be taken into consideration in further studies.[34,40] In addition, the surface may undergo complex reconstructions following the ammonia modification, which could alter the energy landscape substantially and should be a subject of a separate study.

■ CONCLUSIONS

In this work, we have used wet methods to prepare a Si(111) surface terminated predominantly with Si−NH−Si functionality. The FTIR studies showed all the H-terminated reactive sites were substituted after modification with chlorine and later with ammonia. The Si−NH−Si species were identified by FTIR and XPS, which was also used to quantitatively investigate the surface coverages of chlorine and secondary amine. In addition, the XPS spectra suggested that the Si(111) surface remained unoxidized following modification. The surface $Si-NH_x$ species were also identified by ToF-SIMS, and the results were consistent with Si−NH−Si species being dominant. Finally, on the basis of our DFT calculations, the N 1s binding energy detected from XPS was also consistent with the presence of Si−NH−Si surface species. Our initial computational studies suggested that the backbonded Si−NH−Si functionality is the most likely result of the proposed functionalization procedure, and that the first step of the transformation was ammonia reacting with a surface Si−Cl group leading to HCl elimination. Precise characterization of the new approach to preparing $-NH_x$-terminated surfaces will require further studies, both computational and experimental. This newly characterized surface will join the previously established H−Si (111) and Cl−Si (111) surfaces as a general starting point for the preparation of oxygen- and carbon-free interfaces for numerous potential applications.

■ ASSOCIATED CONTENT

Supporting Information. Summary of density functional theory computations on proposed structures, computational investigations of the $Si_{21}H_{28}$ and the $Si_{10}H_{16}$ cluster models, table of fitting parameters for XPS data, and complete reference 69. This material is available free of charge via the Internet at http://pubs.acs.org.

■ AUTHOR INFORMATION

Corresponding Author
andrewt@udel.edu

■ ACKNOWLEDGMENT

This work was supported by the National Science Foundation (CHE-0650123 and CHE-1057374). We also thank Prof. Robert L. Opila and his group in the Department of Materials Science, University of Delaware for the ex situ XPS data collection and useful discussions. The help of Mr. Holt Bui with ToF-SIMS measurements at the Surface Analysis Facility (Department of Chemistry and Biochemistry, University of Delaware) is also gratefully acknowledged.

■ REFERENCES

(1) Aldao, C. M.; Weaver, J. H. *Prog. Surf. Sci.* **2001**, *68*, 189–230.
(2) Sieval, A. B.; Vleeming, V.; Zuilhof, H.; Sudholter, E. J. R. *Langmuir* **1999**, *15*, 8288–8291.
(3) Linford, M. R.; Fenter, P.; Eisenberger, P. M.; Chidsey, C. E. D. *J. Am. Chem. Soc.* **1995**, *117*, 3145–3155.
(4) Cicero, R. L.; Linford, M. R.; Chidsey, C. E. D. *Langmuir* **2000**, *16*, 5688–5695.
(5) Effenberger, F.; Gotz, G.; Bidlingmaier, B.; Wezstein, M. *Angew. Chem., Int. Ed.* **1998**, *37*, 2462–2464.
(6) Sano, H.; Maeda, H.; Ichii, T.; Murase, K.; Noda, K.; Matsushige, K.; Sugimura, H. *Langmuir* **2009**, *25*, 5516–5525.
(7) Boukherroub, R.; Morin, S.; Sharpe, P.; Wayner, D. D. M.; Allongue, P. *Langmuir* **2000**, *16*, 7429–7434.
(8) Buriak, J. M. *Chem. Rev.* **2002**, *102*, 1271–1308.
(9) Leftwich, T. R.; Teplyakov, A. V. *J. Electron Spectrosc. Relat. Phenom.* **2009**, *175*, 31–40.
(10) Perrine, K. A.; Teplyakov, A. V. *Chem. Soc. Rev.* **2010**, *39*, 3256–3274.
(11) Bansal, A.; Li, X. L.; Lauermann, I.; Lewis, N. S.; Yi, S. I.; Weinberg, W. H. *J. Am. Chem. Soc.* **1996**, *118*, 7225–7226.
(12) He, J.; Patitsas, S. N.; Preston, K. F.; Wolkow, R. A.; Wayner, D. D. M. *Chem. Phys. Lett.* **1998**, *286*, 508–514.
(13) Bergerson, W. F.; Mulder, J. A.; Hsung, R. P.; Zhu, X. Y. *J. Am. Chem. Soc.* **1999**, *121*, 454–455.
(14) Bocharov, S.; Dmitrenko, O.; Méndez De Leo, L. P.; Teplyakov, A. V. *J. Am. Chem. Soc.* **2006**, *128*, 9300–9301.
(15) Leftwich, T. R.; Teplyakov, A. V. *J. Phys. Chem. C* **2008**, *112*, 4297–4303.
(16) Bocharov, S.; Mathauser, A. T.; Teplyakov, A. V. *J. Phys. Chem. B* **2003**, *107*, 7776–7782.
(17) Bocharov, S.; Teplyakov, A. V. *Surf. Sci.* **2004**, *573*, 403–412.
(18) Méndez De Leo, L. P.; Teplyakov, A. V. *J. Phys. Chem. B* **2006**, *110*, 6899–6905.
(19) Perrine, K. A.; Leftwich, T. R.; Weiland, C. R.; Madachik, M. R.; Opila, R. L.; Teplyakov, A. V. *J. Phys. Chem. C* **2009**, *113*, 6643–6653.
(20) Kugler, T.; Ziegler, C.; Gopel, W. *Mater. Sci. Eng., B* **1996**, *37*, 112–115.
(21) Bitzer, T.; Alkunshalie, T.; Richardson, N. V. *Surf. Sci.* **1996**, *368*, 202–207.
(22) Rummel, R. M.; Ziegler, C. *Surf. Sci.* **1998**, *418*, 303–313.
(23) Cao, X.; Coulter, S. K.; Ellison, M. D.; Liu, H.; Liu, J.; Hamers, R. J. *J. Phys. Chem. B* **2001**, *105*, 3759–3768.
(24) Mui, C.; Wang, G. T.; Bent, S. F.; Musgrave, C. B. *J. Chem. Phys.* **2001**, *114*, 10170–10180.
(25) Mui, C.; Han, J. H.; Wang, G. T.; Musgrave, C. B.; Bent, S. F. *J. Am. Chem. Soc.* **2002**, *124*, 4027–4038.
(26) Wang, G. T.; Mui, C.; Tannaci, J. F.; Filler, M. A.; Musgrave, C. B.; Bent, S. F. *J. Phys. Chem. B* **2003**, *107*, 4982–4996.
(27) Bent, S. F.; Kachian, J. S.; Rodríguez-Reyes, J. C. F.; Teplyakov, A. V. *Proc. Natl. Acad. Sci. U.S.A.* **2011**, *108*, 956–960.
(28) Shirahata, N.; Hozumi, A.; Yonezawa, T. *Chem. Rec.* **2005**, *5*, 145–159.
(29) Widjaja, Y.; Musgrave, C. B. *Surf. Sci.* **2000**, *469*, 9–20.
(30) Widjaja, Y.; Mysinger, M. M.; Musgrave, C. B. *J. Phys. Chem. B* **2000**, *104*, 2527–2533.
(31) Mathieu, C.; Bai, X. X.; Bournel, F.; Gallet, J. J.; Carniato, S.; Rochet, F.; Sirotti, F.; Silly, M. G.; Chauvet, C.; Krizmancic, D.; et al. *Phys. Rev. B* **2009**, *79*, 205317.
(32) Kubler, L.; Bischoff, J. L.; Bolmont, D. *Phys. Rev. B* **1988**, *38*, 13113–13123.

(33) Owen, J. H. G. *J. Phys.: Condens. Matter* **2009**, *21*, 443001.
(34) Rodríguez-Reyes, J. C. F.; Teplyakov, A. V. *Phys. Rev. B* **2007**, *76*, 075348.
(35) Bowler, D. R.; Owen, J. H. G. *Phys. Rev. B* **2007**, *75*, 155310.
(36) Chung, O. N.; Kim, H.; Chung, S.; Koo, J. Y. *Phys. Rev. B* **2006**, *73*, 033303.
(37) Rangelov, G.; Stober, J.; Eisenhut, B.; Fauster, T. *Phys. Rev. B* **1991**, *44*, 1954–1957.
(38) Kim, Y. S.; Koo, J. Y.; Kim, H. *Phys. Rev. Lett.* **2008**, *100*, 256105.
(39) Kim, Y. S.; Koo, J. Y.; Kim, H. *J. Phys.: Condens. Matter* **2009**, *21*, 064237.
(40) Rodríguez-Reyes, J. C. F.; Teplyakov, A. V. *Phys. Rev. B* **2008**, *78*, 165314.
(41) Dai, M.; Wang, Y.; Kwon, J.; Halls, M. D.; Chabal, Y. J. *Nat. Mater.* **2009**, *8*, 825–830.
(42) Ziegenbalg, G.; Focke, T.; Holldorf, H. *J. Mater. Sci.* **1999**, *34*, 2199–2206.
(43) Liu, D.; Lv, Q.; Yu, J. Q. Method for producing hexamethyldisilazane. DE Patent WO/2001/012636, February 22, 2001.
(44) Ackerhans, C.; Räke, B.; Krätzner, R.; Müller, P.; Roesky, H. W.; Usón, I. *Eur. J. Inorg. Chem.* **2000**, *2000*, 827–830.
(45) Passarelli, V.; Carta, G.; Rossetto, G.; Zanella, P. *Dalton Trans.* **2003**, *2003*, 413–419.
(46) Sheludyakov, V. D.; Lebedeva, A. B.; Shukyurov, A. K.; Kirilin, A. D. *Zh. Obshch. Khim.* **1986**, *56*, 1308–1311.
(47) Chen, X.; Zhou, X. Z. *Acta Chim. Sin.* **1984**, *42*, 479–486.
(48) Zhdanov, A. A.; Kotrelev, G. V.; Kazakova, V. V.; Redkozubova, Y. P. *Vysokomol. Soedin., Ser. A* **1985**, *27*, 1422–1427.
(49) Varezhkin, Y. M.; Mikhailova, A. N.; Krasnova, T. L.; Chernyshev, E. A. *Russ. J. Gen. Chem.* **2004**, *74*, 1513–1519.
(50) Low, M. J. D.; Severdia, A. G.; Chan, J. *J. Catal.* **1981**, *71*, 144–151.
(51) Bagatur'yants, A. A.; Novoselova, K. P.; Safonov, A. A.; Savchenko, L. L.; Cole, J. V.; Korkin, A. A. *Mater. Sci. Semicond. Proc.* **2000**, *3*, 23–29.
(52) Finstad, C. C.; Thorsness, A. G.; Muscat, A. J. *Surf. Sci.* **2006**, *600*, 3363–3374.
(53) Lange, B.; Schmidt, W. G. *Science* **2008**, *602*, 1207–1211.
(54) Soria, F. A.; Patrito, E. M.; Paredes-Olivera, P. *Langmuir* **2011**, *27*, 2613–2624.
(55) Higashi, G. S.; Chabal, Y. J.; Trucks, G. W.; Raghavachari, K. *Appl. Phys. Lett.* **1990**, *56*, 656–658.
(56) Zhang, X.; Garfunkel, E.; Chabal, Y. J.; Christman, S. B.; Chaban, E. E. *Appl. Phys. Lett.* **2001**, *79*, 4051–4053.
(57) Royea, W. J.; Juang, A.; Lewis, N. S. *Appl. Phys. Lett.* **2000**, *77*, 1988–1990.
(58) Bansal, A.; Li, X. L.; Yi, S. I.; Weinberg, W. H.; Lewis, N. S. *J. Phys. Chem. B* **2001**, *105*, 10266–10277.
(59) Rivillon, S.; Chabal, Y. J.; Webb, L. J.; Michalak, D. J.; Lewis, N. S.; Halls, M. D.; Raghavachari, K. *J. Vac. Sci. Technol. A* **2005**, *23*, 1100–1106.
(60) Baier, M.; Bissinger, P.; Schmidbaur, H. *Z. Naturforsch., Sect. B* **1993**, *48*, 1672–1674.
(61) Bai, G. C.; Müller, P.; Roesky, H. W.; Usón, I. *Organometallics* **2000**, *19*, 4675–4677.
(62) Mori, A.; Mohamed-Ahmed, M. S.; Sekiguchi, A.; Masui, K.; Koike, T. *Chem. Lett.* **2002**, *2002*, 756–757.
(63) Hassan, S.; Hector, A. L.; Hyde, J. R.; Kalaji, A.; Smith, D. C. *Chem. Commun.* **2008**, *42*, 5304–5306.
(64) Kern, W. *J. Electrochem. Soc.* **1990**, *137*, 1887–1892.
(65) Briggs, D.; Seah, M. P. *Practical Surface Analysis: Auger and X-ray Photoelectron Spectroscopy*, 2nd ed.; Wiley: New York, 1990; Vol. 1.
(66) Haber, J. A.; Lewis, N. S. *J. Phys. Chem. B* **2002**, *106*, 3639–3656.
(67) Webb, L. J.; Nemanick, E. J.; Biteen, J. S.; Knapp, D. W.; Michalak, D. J.; Traub, M. C.; Chan, A. S. Y.; Brunschwig, B. S.; Lewis, N. S. *J. Phys. Chem. B* **2005**, *109*, 3930–3937.
(68) Greenwood, N. N.; Earnshaw, A. *Chemistry of the Elements*, 2nd ed.; Butterworth-Heinemann Limited: Oxford, UK, 1997; p 1600.
(69) Frisch, M. J. T.; et al. . *Gaussian 09*, Revision B.01, Gaussian, Inc.: Wallingford, CT, 2009.
(70) Becke, A. D. *J. Chem. Phys.* **1993**, *98*, 1372–1377.
(71) Krishnan, R.; Binkley, J. S.; Seeger, R.; Pople, J. A. *J. Chem. Phys.* **1980**, *72*, 650–654.
(72) Lee, C. T.; Yang, W. T.; Parr, R. G. *Phys. Rev. B* **1988**, *37*, 785–789.
(73) McLean, A. D.; Chandler, G. S. *J. Chem. Phys.* **1980**, *72*, 5639–5648.
(74) Queeney, K. T.; Chabal, Y. J.; Raghavachari, K. *Phys. Rev. Lett.* **2001**, *86*, 1046–1049.
(75) González, J. A.; de la Fuentá, I. G.; Cobos, J. C. *Fluid Phase Equilib.* **2000**, *168*, 31–58.
(76) Maity, T.; Samanta, B. C.; Banthia, A. K. *J. Appl. Polym. Sci.* **2008**, *110*, 3717–3726.
(77) Dillon, A. C.; Gupta, P.; Robinson, M. B.; Bracker, A. S.; George, S. M. *J. Vac. Sci. Technol. A* **1991**, *9*, 2222–2230.
(78) Bater, C.; Sanders, M.; J. H. Craig, J. *Surf. Interface Anal.* **2000**, *29*, 208–214.
(79) Bischoff, J. L.; Lutz, F.; Bolmont, D.; Kubler, L. *Surf. Sci.* **1991**, *251*, 170–174.
(80) Webb, L. J.; Lewis, N. S. *J. Phys. Chem. B* **2003**, *107*, 5404–5412.
(81) Toyoda, S.; Okabayashi, J.; Kumigashira, H.; Oshima, M. *Appl. Phys. Lett.* **2005**, *87*, 102901.
(82) Matsuoka, M.; Isotani, S.; Sucasaire, W.; Zambom, L. S.; Ogata, K. *Surf. Coat. Technol.* **2010**, *204*, 2923–2927.
(83) Lee, C. Y.; Harbers, G. M.; Grainger, D. W.; Gamble, L. J.; Castner, D. G. *J. Am. Chem. Soc.* **2007**, *129*, 9429–9438.
(84) Colaianni, M. L.; Chen, P. J.; Yates, J. T., Jr. *J. Chem. Phys.* **1992**, *96*, 7826–7837.
(85) Bjorkqvist, M.; Gothelid, M.; Grehk, T. M.; Karlsson, U. O. *Phys. Rev. B* **1998**, *57*, 2327–2333.